

# Path Planning of a 3-UPU Wrist Manipulator for Sun Tracking in Central Receiver Tower Systems

R.B. Ashith Shyam<sup>1</sup>, Ghosal A<sup>2,\*</sup>

---

## Abstract

Heliostats capable of tracking the sun as it moves across the sky and focusing the incident solar energy on to a central receiver tower requires a two degree-of-freedom (DOF) mechanism which can orient the mirror in the desired manner. Existing two-DOF mechanism, such as the Azimuth-Elevation (Az-EL) and the Target-Aligned (T-A), have two actuators in series. It is known that during certain times of the day, the T-A configuration has less spillage losses and astigmatic aberration while at other times the Az-El configuration is better. In this paper, we propose a three-DOF parallel manipulator which can be used as a heliostat. The proposed 3-UPU, three-DOF parallel manipulator, has a fixed point about which the mirror can rotate about three axes. Since only two DOF are required to track the sun, the 3-UPU is a redundant system. We propose a strategy to use this redundancy and electronically reconfigure the 3-UPU to achieve the Az-El and T-A configurations thus achieving the advantages of both. As the motion of the sun is precisely known for a known location, time and day of the year, numerical simulations done a priori provide the conditions for switching.

*Keywords:* Heliostat, 3-UPU wrist, Sun tracking, Parallel manipulator, Central receiver, PID control

---

## 1. Introduction

From the time parallel manipulators were first introduced by Gough [1] and Stewart [2], it has been known that they provide high structural rigidity and more accurate positioning and orientation of the end-effector or the moving platform[3]. The increased rigidity is due to the fact that the moving platform  
5 is supported at multiple points thereby the external load is shared. The increased accuracy is due to the fact that the positioning and pointing error of

---

\*Corresponding author

*Email addresses:* shyamashi@gmail.com (R.B. Ashith Shyam ),  
asitava@mecheng.iisc.ernet.in (Ghosal A)

*URL:* <http://www.mecheng.iisc.ernet.in/~asitava/> (Ghosal A)

<sup>1</sup>Research Scholar, Mechanical Engineering, Indian Institute of Science, Bangalore

<sup>2</sup>Professor, Mechanical Engineering, Indian Institute of Science, Bangalore

the end-effector is a function of the largest error in any actuator and *not* the sum of the errors as in a serial arrangement. Due to these inherent advantages, parallel manipulators have been extensively used in flight simulators, precision manufacturing, pointing devices, medical applications, and, more recently, in video games. In harvesting solar energy, one approach is to reflect the incident solar radiation by mirrors on to a stationary central receiver (CR). At the central receiver, the reflected solar thermal radiation from several such mirrors are converted to electricity. As the Earth rotates during the day and around the sun, the sun traces a well-defined path in the sky and to continuously reflect the solar radiation, the mirror has to rotate about two axis. The device including the mirror and the actuators required to rotate the mirror assembly is called a heliostat and traditionally the two rotation axis of a heliostat and the two actuators are in series. In the well-known Azimuth-Elevation (Az-El) arrangement, as the name implies, the mirror is rotated about the elevation and the azimuth axis. In another configuration, the mirror is rotated about a line connecting the mirror centre to the stationary receiver centre and about the elevation – this is known as the Target-Aligned (T-A) or the Spinning-Elevation arrangement. The pointing accuracy requirement for a typical heliostat is 2-3 mrad and the heliostat is expected to track the sun in the presence of wind and gravity loading (see reference [4] for more details on heliostat and sun tracking). Meeting these requirements, in a CR system with thousands of heliostats, results in the cost of the heliostats of about 40-50% of the total installation cost [5]. Hence, attempts are being made worldwide to reduce the cost of the heliostat so as to make a CR system competitive with other ways to harvest incident solar energy. Due to the inherent advantages of increased structural rigidity, a platform type parallel manipulator can carry larger mirror or require less structural supporting material to main the required low deformation. Due to the inherent increased positioning and orientation accuracy in a platform type parallel manipulator, it is expected that the required pointing accuracy can be more easily satisfied or cheaper less accurate actuators can be used to achieve the required pointing accuracy. Both these aspects can lead to reduction in cost of a heliostat and this is main motivation behind using a platform type manipulator over the traditional serial Az-El and T-A configuration heliostats. In this paper, we propose the use of a three-degree-of-freedom parallel manipulator for sun tracking in concentrated solar power systems.

There have been a few attempts to use parallel manipulators in sun tracking. In the work by [6], a two degree-of-freedom parallel manipulator called the U-2PUS has been developed for photo-voltaic (PV) systems. The author claims that this manipulator is ideal for photo-voltaic systems in latitudes from 0 to 50°. This parallel manipulator could be used for photo-voltaic systems but cannot be used for central receiver (CR) systems since in a field with photo-voltaic panels, all the PV panels are tracked in a similar manner. There is no reflection of the incident solar radiation and the conversion to electricity takes place in the PV panel itself. The location of the PV panels in the field do not play any part as the Sun's rays are parallel everywhere. For central receiver systems, the heliostats at different locations in the field will have different motion if the

incident energy is to be reflected to a central receiver. Mathematically, it can  
55 be shown that there are more unknowns than equations available in the U-  
2PUS parallel manipulator system and hence it cannot be used in a CR system.  
A four degree-of-freedom parallel manipulator is proposed for sun-tracking in  
[7]. In this work, the collector which is initially kept high above the ground is  
allowed to fall down in a controlled manner under the influence of gravity thereby  
60 attaining the required orientation. One major drawback of this manipulator is  
that it casts its own shadow on the collector and no prototype has been made  
to check the veracity of the claims. Google’s Heliostat Optical Simulation Tool  
(HOpS) [8] is an attempt to do sun tracking in CR systems by the use of cable  
attached mirrors. Although there are some advantages to the system, this can  
65 be used only in places where the wind speeds are very low. Several other two  
degree-of-freedom (DOF) spherical mechanisms (see references [9, 10, 11, 12])  
for application specific purposes such as camera orientation, scanning spherically  
shaped items etc. are described in literature but none of these have been shown  
to be capable of tracking the sun for central receiver systems.

70 A new type of tracking strategy which is independent of latitude has been  
proposed in [13]. The authors claim to have introduced some advantages in  
mechatronic control schemes, high optical efficiency by operating the heliostat  
at a very narrow range of incident angles. Another interesting strategy called  
an integer linear programming is developed for optimizing the aiming strategy  
75 [14] and thus to control the spike on the receiver aperture temperature thereby  
preventing its damage. The pitch-roll and slope-drive tracking (see references  
mechanisms [15, 16, 17, 18]) are gaining popularity and has been employed in  
the CSIRO and Stello heliostats.

In this work, the focus is on CR systems and we propose a parallel manip-  
80 ulator, viz., the 3-UPU wrist that can be used for sun tracking in CR systems  
without any of the above mentioned disadvantages. The ‘U’ denotes a two-DOF  
Hooke joint, the ‘P’ denotes single DOF a prismatic or sliding joint. In the par-  
allel manipulator, the ‘P’ joint is actuated and the other joints are not actuated  
or are passive. In addition, the 3-UPU can be reconfigured to be used either in  
85 Azimuth-Elevation (Az-El) or in the Target-Aligned (T-A or spinning-elevation)  
method thus combining the advantages of both by simply changing software and  
control strategy and *does not* require any change in the hardware. The 3-UPU  
wrist can thus be operated in a mode which gives the best performance in terms  
of spillage losses or astigmatism at a particular time of the day or a date in the  
90 year. In the parallel configuration, linear actuators are used. The motion of  
the prismatic (P) joints or the stroke of the linear actuators are computed using  
inverse kinematics algorithms and adjusted with respect to time to achieve the  
orientation required for sun tracking. The parallel manipulator requires three  
actuators as opposed to two in the Az-El and T-A configurations. However,  
95 since the support material is less [19] or larger mirrors can be used and less  
expensive and less accurate linear actuators can be used, the overall cost of the  
plant is expected to be less.

The paper is organized as follows: Section 2 gives the kinematics of the 3-  
UPU wrist and the rotation matrix for both the Az-EL and T-A heliostat are

100 obtained. From a desired rotation matrix, the actuations at the P joints are computed. In section 3, simulations carried out for Bangalore and Rajasthan, India on the feasibility of using a 3-UPU wrist as a sun tracker in CR systems is presented. Section 4 shows the prototype design, the controller used, the results from actual sun tracking experiments performed and the observations made during the experiment. Finally, section 5 summarizes the work done and gives an insight into the future directions of research.

## 2. Kinematics of the 3-UPU wrist manipulator

Section 2 (a) shows a CAD model of the 3-UPU wrist manipulator. The 3-UPU manipulator has a bottom platform (fixed base) and a top moving platform connected together by three legs having joints in the order universal-prismatic-universal (UPU). The conditions which have to be satisfied for making a 3-UPU manipulator to be a wrist are listed in [20] and the kinematics equations of the 3-UPU wrist manipulator is given in reference[21]. Section 2 (b) shows a close-up view of a leg.

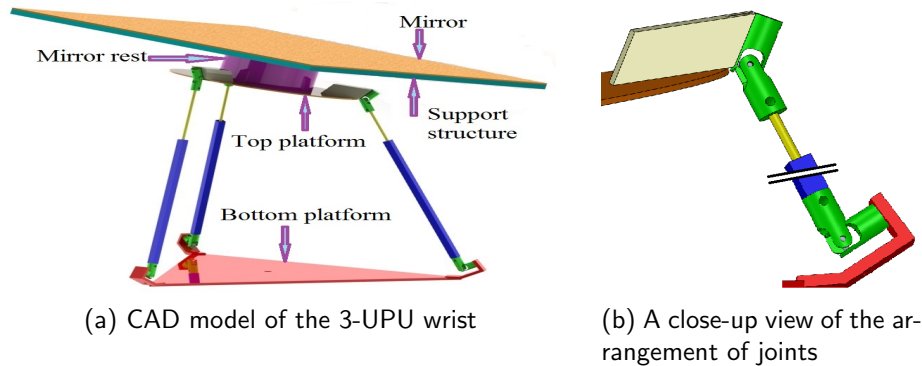


Fig. 1: The 3-UPU heliostat and its joints

115 The 3-UPU wrist manipulator is capable of performing finite spherical motions about the fixed wrist point when the prismatic joints are actuated. For sun tracking, the fixed point should be carefully chosen so that it falls above the top moving platform. As shown in section 2 (a), by using suitable attachments labeled as mirror rest, the mirror centre and the fixed point are made to coincide with each other. This design makes the mirror rotate about the fixed point just like in a serial Az-El or T-A arrangements as one can make two consecutive Euler rotations about a point for sun tracking.

120 The schematic diagram of the 3-UPU wrist manipulator is shown in Fig 2. The global or fixed co-ordinate system with its origin at  $O$  has axes  $OX$ ,  $OY$  and  $OZ$  pointing towards local East, local North and Zenith directions, respectively. The  $Z$  axis of the global co-ordinate system passes through the centre of the vertical receiver tower. The base co-ordinate system,  $\{B\}$  having axes  $x_b$ ,  $y_b$

and  $z_b$  has its origin at  $O_1$  and is at a radius  $R$  from  $O$  and at an angle  $\psi$  with respect to the  $OX$  axis. The co-ordinate system at the top platform,  $\{M\}$ , has its origin at wrist point  $G$  and has axes  $x_m, y_m$  and  $z_m$ . The symbols  $U_{bi}$  and  $U_{ti}$  ( $i = 1, 2, 3$ ) denote the universal joints at the base and top, respectively. Without loss of generality, the triangles formed by  $U_{bi}$  and  $U_{ti}$  can be considered to be equilateral triangles whose circum-radii are  $r_b$  and  $r_p$ , respectively. The degrees of freedom of the manipulator can be found out by using the well-known Grübler - Kutzbach criterion

$$DOF = \lambda(N - J - 1) + \Sigma F_i, \quad (1)$$

where  $\lambda$  is 6 for spatial and 3 for planar motion,  $N$  is the number of links including the fixed link,  $J$  is the number of joints and  $F_i$  is the degrees of freedom of the  $i^{\text{th}}$  joint. The DOF of the 3-UPU manipulator computed from Eqn. (1) is found to be 3 or in other words three actuators are needed to obtain arbitrary desired orientation of the top moving platform.

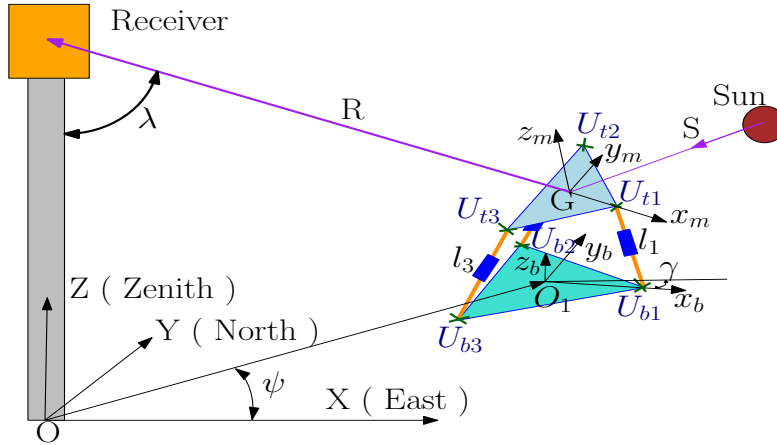


Fig. 2: Schematic of the 3-UPU manipulator and receiver

From the latitude, longitude and the location of the heliostat in the field and the time and day of the year, the sun vector  $\vec{GS}$  or the ray pointing towards the sun can be found out. The vector denoting the reflected ray from  $G$  to the receiver center  $\vec{GR}$  is also known. From the laws of optics, the normal to the mirror, denoted by  $\vec{GN}$ , can be written as

$$\vec{GN} = \frac{\vec{GS} + \vec{GR}}{\|\vec{GS} + \vec{GR}\|} \quad (2)$$

Once the mirror normal is known, we can obtain the rotation matrix describing the orientation of the mirror co-ordinate system  $\{M\}$  with respect to the fixed co-ordinate system  $\{B\}$ . Denoting the rotation matrix by  ${}^M_B[R]$ , we can write

in general

$${}^M_B[R] = \begin{bmatrix} n_1 & o_1 & a_1 \\ n_2 & o_2 & a_2 \\ n_3 & o_3 & a_3 \end{bmatrix} \quad (3)$$

we observe that the column vector  $(a_1, a_2, a_3)^T$  is the mirror normal  $\overrightarrow{GN}$  and is known. To obtain the other two columns for the Azimuth-Elevation (Az-El) and Target-Aligned (T-A) configurations, we use the properties of the rotation matrix and the two consecutive Euler rotations used in these two sun tracking schemes. This is discussed next.

### 2.1. Rotation matrix for Az-El heliostat

The nominal orientation of the mirror is parallel to the ground, i.e., the axes  $x_m$ ,  $y_m$  and  $z_m$  are parallel to  $OX$ ,  $OY$  and  $OZ$ , respectively. As the sun moves across the sky, the two consecutive Euler rotations required to track sun and reflect the rays to the receiver are

1. Rotation about  $Z$  by an angle  $\theta_{Az}$  where  $\theta_{Az}$  is the angle made by the projection of heliostat normal with the  $X$  axis.
2. Rotation about  $y_m$  by an angle  $(\frac{\pi}{2} - \theta_{El})$  where  $\theta_{El}$  is the angle made by the heliostat normal with the ground plane.

Hence, the rotation matrix becomes

$$R_{Az-El} = \begin{bmatrix} \cos \theta_{Az} \sin \theta_{El} & -\sin \theta_{Az} & \cos \theta_{Az} \cos \theta_{El} \\ \sin \theta_{Az} \sin \theta_{El} & \cos \theta_{Az} & \sin \theta_{Az} \cos \theta_{El} \\ -\cos \theta_{El} & 0 & \sin \theta_{El} \end{bmatrix} \quad (4)$$

In the Az-El sun tracking the  $y_m$  axis of the mirror coordinate system would still lie on a plane parallel to the  $X - Y$  plane and as a result the (3,2) element of the rotation matrix,  $R_{Az-El}$ , is zero. It may be noted that the third column is same as mirror normal  $\overrightarrow{GN}$  (see Eqn. (2)) with direction cosines  $a_1, a_2, a_3$  and is known. Equating the (3,3) element with the known  $a_3$ , we obtain  $\theta_{El}$ . Similarly and equating (3,1) and (3,2) element with  $a_1$  and  $a_2$ , respectively and using the four-quadrant tangent inverse (Atan2) function, we can obtain  $\theta_{Az}$ . Once the  $\theta_{El}$  and  $\theta_{Az}$  angles are known, we can obtain all the other elements of the rotation matrix  ${}^M_B[R]$  in Eqn.(3).

### 2.2. Rotation matrix for T-A heliostat

The target aligned (T-A) equations for sun tracking have been developed and are available (see references [22, 23, 24]). In the T-A configuration, one of the axes of rotation will be coincident with the reflected ray  $\overrightarrow{GR}$  and the other axis is perpendicular to the reflected ray and lies in the plane of the mirror. Thus the heliostat spins about  $\overrightarrow{GR}$  by  $\theta_{sp}$  (spinning angle) and rotates about  $y_m$  by

$\theta_{el}$  (elevation angle). From the nominal orientation, parallel to the ground, two Euler rotations have to be performed initially, the first about  $Z$  axis by an angle  $\psi$  and then about  $y_m$  by an angle  $-\lambda$ . After these two consecutive rotations, the normal to the mirror and the reflected ray will become coincident. The rotation matrix for the T-A heliostat is given by

$$\begin{bmatrix} c_\psi c_\lambda c_{\theta_{sp}} c_{\theta_{el}} - s_\psi s_{\theta_{sp}} c_{\theta_{el}} + c_\psi s_\lambda s_{\theta_{el}} & -c_\psi c_\lambda s_{\theta_{sp}} - s_\psi c_{\theta_{sp}} & c_\psi c_\lambda c_{\theta_{sp}} s_{\theta_{el}} - s_\psi s_{\theta_{sp}} s_{\theta_{el}} - c_\psi s_\lambda c_{\theta_{el}} \\ s_\psi c_\lambda c_{\theta_{sp}} c_{\theta_{el}} + c_\psi s_{\theta_{sp}} c_{\theta_{el}} + s_\psi s_\lambda s_{\theta_{el}} & -s_\psi c_\lambda s_{\theta_{sp}} + c_\psi c_{\theta_{sp}} & s_\psi c_\lambda c_{\theta_{sp}} s_{\theta_{el}} + c_\psi s_{\theta_{sp}} s_{\theta_{el}} - s_\psi s_\lambda c_{\theta_{el}} \\ s_\lambda c_{\theta_{sp}} c_{\theta_{el}} - c_\lambda s_{\theta_{el}} & -s_\lambda s_{\theta_{sp}} & s_\lambda c_{\theta_{sp}} s_{\theta_{el}} + c_\lambda c_{\theta_{el}} \end{bmatrix} \quad (5)$$

where  $c_{(\cdot)}, s_{(\cdot)}$  represents the cosine and sine of the respective angles  $(\cdot)$ . As in the Az-El heliostat, the normal  $\overrightarrow{GN}$  and hence the third column of the rotation matrix is known. The angles  $\psi$  and  $\lambda$  (see Fig 2) are also known from the prior knowledge of heliostat location in the field. Equating  $a_1, a_2$  and  $a_3$  with the elements of the last column matrix given in Eqn.(5), we can obtain the angles  $\theta_{sp}$  and  $\theta_{el}$  by inverse trigonometric functions. Once the two angles are known all the elements in the first and second columns of the rotation matrix  ${}^M_B[R]$  can be computed.

### 2.3. Actuations required for the 3-UPU wrist

As mentioned earlier, the top-platform and the mirror are connected together using an attachment such that the orientation of both are the same with respect to the base. The only difference being the centre of the mirror remains at the fixed point even while executing finite spherical rotations whereas it is not the same for the top platform. Initially, both the top and bottom platforms are assumed to be parallel. Then the rotation which takes the mirror to the base is found out as mentioned in sections 2.1 and 2.2. The centre of the top platform will be at a constant distance from the mirror centre in its normal direction downwards. Using this information, the centre of the top platform is found out and hence the actuation required for the legs of 3-UPU wrist can be found out as follows:

For the 3-UPU manipulator with the base and top platform assumed to be equilateral triangles, the co-ordinates of the  $U_{bi}$  joints with respect to  $\{B\}$  are given by

$$\begin{aligned} \overrightarrow{O_1U_{b1}} &= (r_b, 0, 0)^T \\ \overrightarrow{O_1U_{b2}} &= \left(-\frac{1}{2}r_b, \frac{\sqrt{3}}{2}r_b, 0\right)^T \\ \overrightarrow{O_1U_{b3}} &= \left(-\frac{1}{2}r_b, -\frac{\sqrt{3}}{2}r_b, 0\right)^T \end{aligned} \quad (6)$$

175 and the co-ordinates of the  $U_{ti}$  joints with respect to  $\{x_m, y_m, z_m\}$  are given by

$$\begin{aligned}
 \overrightarrow{GU_{t1}} &= (r_p, 0, 0)^T \\
 \overrightarrow{GU_{t2}} &= \left(-\frac{1}{2}r_p, \frac{\sqrt{3}}{2}r_p, 0\right)^T \\
 \overrightarrow{GU_{t3}} &= \left(-\frac{1}{2}r_p, -\frac{\sqrt{3}}{2}r_p, 0\right)^T
 \end{aligned} \tag{7}$$

The position vector of the top U joints with respect to the base co-ordinate system  $\{B\}$  is given as

$$\begin{bmatrix} \overrightarrow{O_1U_{ti}} \\ 1 \end{bmatrix} = [T] \begin{bmatrix} \overrightarrow{GU_{ti}} \\ 1 \end{bmatrix}$$

where  $[T]$  is the  $4 \times 4$  transformation matrix which relates the mirror  $\{M\}$  to the base co-ordinate system  $\{B\}$ . The  $3 \times 3$  rotation matrix is  ${}^M_B[R]$  in  $[T]$  can be obtained for the Az-El and T-A configurations ( see section 2.1 and section 2.2) as the sun moves across the sky and the last column of  $[T]$  contains the position vector of the fixed wrist point G.

180 The leg lengths or the actuation needed to obtain  ${}^M_B[R]$  can be found out as [25]

$$l_i = \|\overrightarrow{O_1U_{bi}} - \overrightarrow{O_1U_{ti}}\|, \quad i = 1, 2, 3 \tag{8}$$

where  $\|A\|$  represents the norm of the vector described by  $A$  and  $U_{ti}$  and  $U_{bi}$  ( $i = 1, 2, 3$ ) are given in Eqns. (7) and (8), respectively.

### 3. Simulation results for 3-UPU wrist

Extensive simulations have been carried out to prove that the 3-UPU wrist can indeed work in both Az-El and T-A modes. To perform the simulations a program has been developed for carrying out the simulation study for any location on the Earth's surface and for any day. For illustrative purposes, we show simulations carried out for Bangalore ( $12^\circ 58' 13''$  N,  $77^\circ 33' 37''$  E) and Rajasthan ( $26^\circ 42' 58''$  N,  $75^\circ 41' 44''$  E) for four days, viz., March equinox, summer solstice, September equinox and winter solstice. These four days represent the extremes of the angular tilt of the earth's rotational axis with respect to the incoming sun rays. The height of the receiver tower varies from 43 m (IEA-CRS, Spain) to 195 m (Crescent Dunes, USA) [4]. For simulations we assume that the centre of the receiver aperture to be at a location  $[0 \ 0 \ 65]^T$  m with respect to the global co-ordinate system. Although the distance of the heliostats from the tower in a surround solar field varies from a few meters to as large as a kilometer, we present the simulation results for a heliostat placed at a radial distance of 100 m and at an angle of  $30^\circ$  with the local East axis. The fixed point of the 3-UPU wrist is assumed to be at a height of 2 m from the bottom platform. The mirror and the receiver aperture are assumed to have a dimension of  $2 \text{ m} \times 2 \text{ m}$  and

200



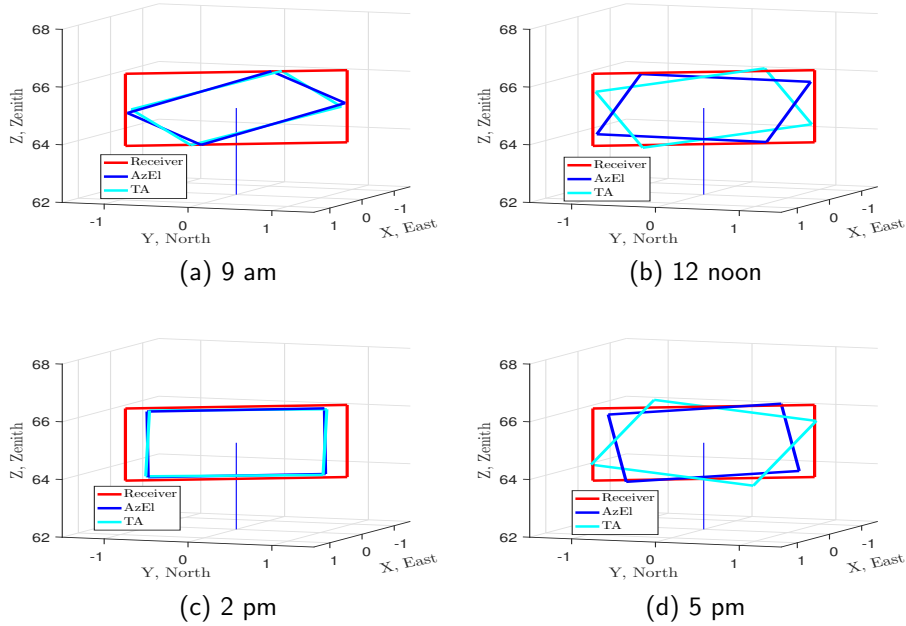


Fig. 3: The image on the receiver aperture at various time instants for March equinox for Bangalore

2.5 m  $\times$  2.5 m, respectively. These numbers are chosen since dimensions more a few meters would be difficult to handle for prototyping and proof of concept.

For the simulations, the following assumptions are made:

- The effect of atmospheric conditions like dust and other particles which reflect and scatter the sun rays are negligible,
- The mirrors are perfectly flat, and
- At every instant of time, the sun ray hitting the centre of the mirror goes to the centre of the receiver aperture.

From the above assumption, the ray hitting the corners of the mirror will be reflected parallel to the central ray and by tracing this ray on the receiver aperture, we can obtain the image formed at the receiver. This plot of the image on the receiver plane for a 3-UPU wrist working in Az-EL and T-A methods are shown in Fig 3. Fig 4 shows the simulation results for various time instants for March equinox in Bangalore if the 3-UPU wrist manipulator is to be used in T-A method. It is can be seen from Fig 4d that the legs of the 3-UPU wrist intersect each other during the evening time. In order to prevent this, the rotation matrix obtained using T-A method can be multiplied by a rotation about the mirror normal so that the legs of the 3-UPU will not

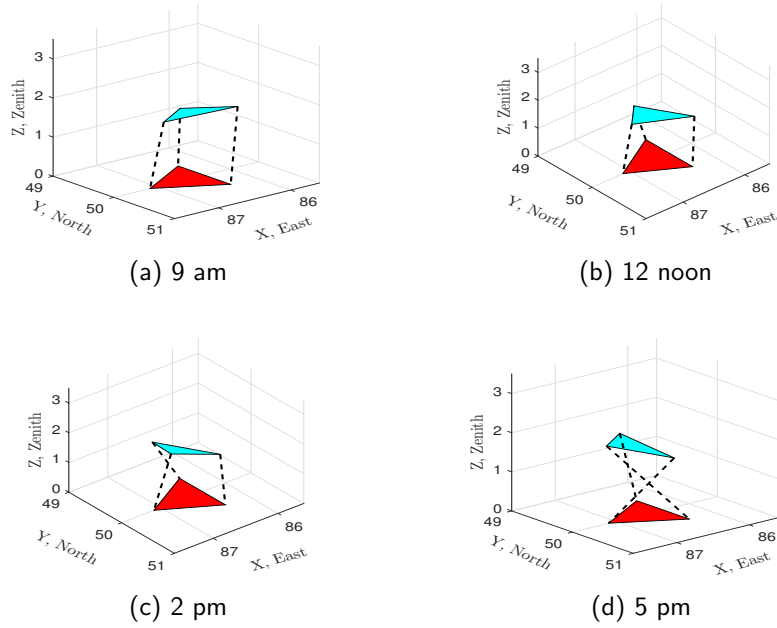


Fig. 4: Simulation of 3-UPU wrist for T-A mode for March equinox for Bangalore

intersect. Fig 5 shows the modified simulation results when the T-A rotation matrix is multiplied by another rotation about mirror normal by  $60^\circ$ .

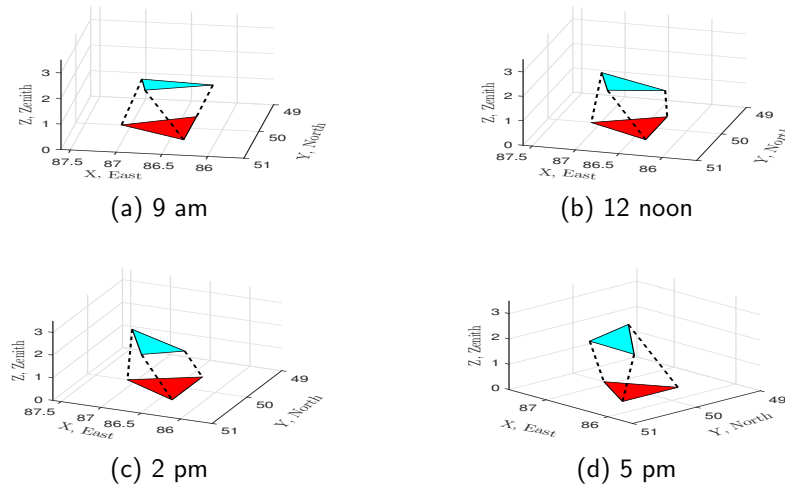


Fig. 5: Simulation of 3-UPU wrist for modified T-A mode for March equinox for Bangalore

The actuations required for T-A and modified T-A are given in Fig 6.

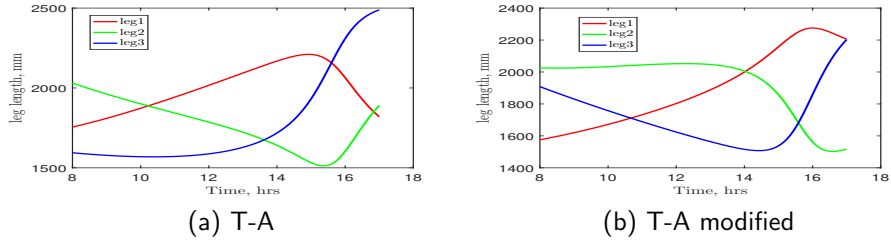


Fig. 6: Actuations required for 3-UPU wrist for March equinox for Bangalore

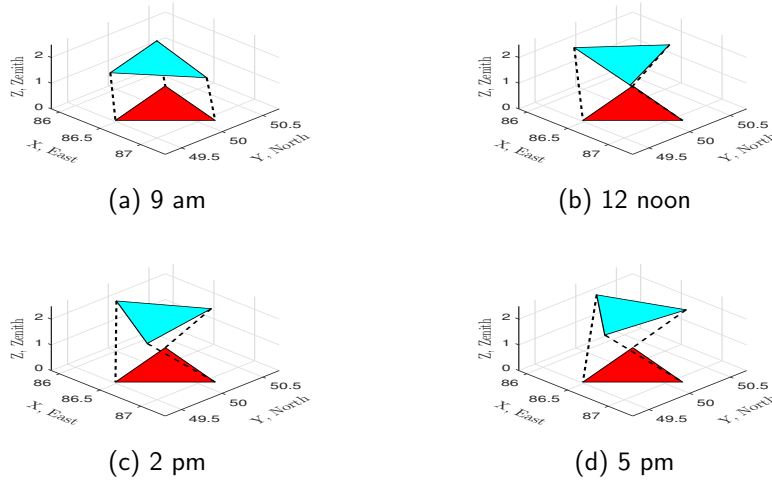


Fig. 7: Simulation of 3-UPU wrist for modified Az-El mode for summer solstice for Rajasthan

Similarly, Fig 7 gives the simulation results obtained for modified Az-El method

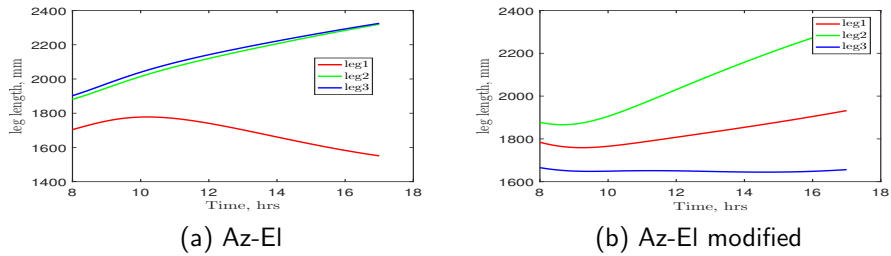


Fig. 8: Actuations required for 3-UPU wrist in Az-El mode for summer solstice for Rajasthan

for summer solstice in Rajasthan. Here, the Az-El rotation matrix is multiplied with another rotation of  $90^\circ$  about the mirror normal to avoid intersection of the legs. Fig 8 gives the actuation required for the 3-UPU heliostat in Az-El method in normal operation and when modified.

### 3.1. Spillage loss for 3-UPU wrist

From Fig 3, it can be seen that at some instants of time, the image goes out of the receiver aperture and this is often called as spillage loss. Fig 9 shows the spillage loss for various days for Bangalore. From these plots it is possible to find out at what time instant the switch from Az-El to T-A or vice-versa should be carried out from the point of view of reducing the spillage loss. As an example, for the March equinox (Fig 9a) and for the heliostat located as mentioned above, the spillage loss in the T-A mode is less till 10:50 a.m. and for June solstice till 12:40 p.m. Before these times the sun tracking can be done in the T-A mode and after these times the sun tracking should be switched to the Az-El mode. The analysis shown is for Bangalore, however similar simulations and analysis can be carried out for any other location on the Earth's surface and at any location in the heliostat field.

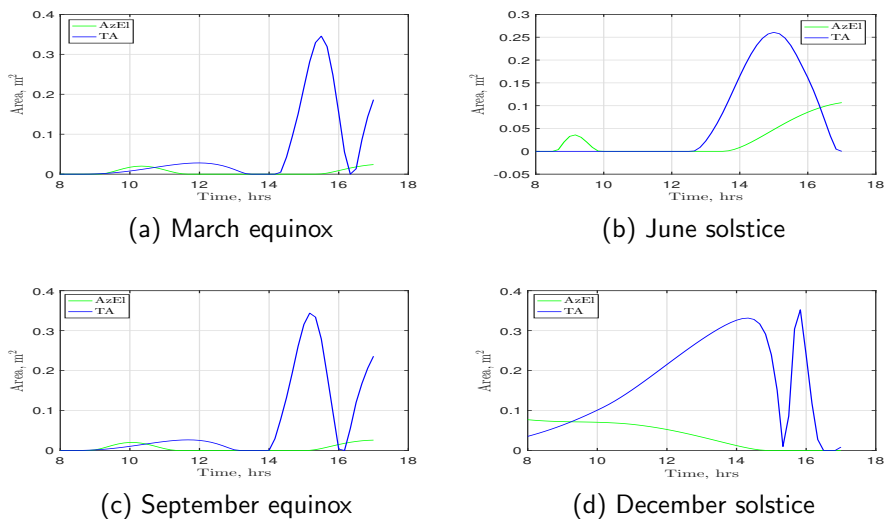


Fig. 9: Spillage loss for 3-UPU wrist for Bangalore

## 4. Experimental validation

To validate the numerical simulation results, we fabricated a prototype 3-UPU wrist based heliostat. The design of the prototype, the controller developed for actuating the P joints and the experimental results obtained are presented in this section.

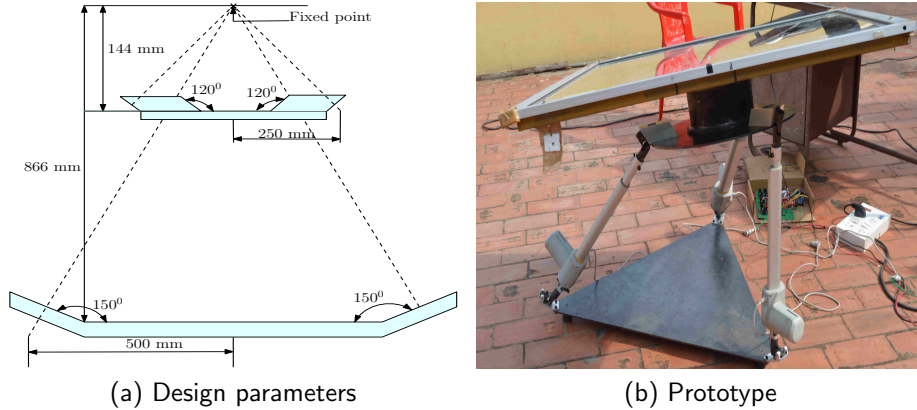


Fig. 10: The design parameters and the prototype of the 3-UPU wrist

Fig 10(a) shows some of the main dimensions of the designed prototype and Fig 10 (b) shows a photograph of the fabricated prototype. With reference to Fig 10, the circum radii of the bottom and top platforms are chosen as 500 mm and 250 mm, respectively. The bottom platform which is equilateral, is attached with a  $150^\circ$  angle section at its corners. The U-joints are attached to this section thus giving the fixed point at a distance of 866 mm from the bottom. Similarly, the top platform has a  $120^\circ$  angle section attached to it. The mirror and the top platform are connected together using a cylindrical mirror rest. The mirror rest has a diameter of 220 mm and a height of 138 mm. The mirror which has a dimension of  $1\text{ m} \times 1\text{ m}$  is supported at its back by a support structure to prevent it from excessive deflection due to wind loading or self-weight. The mirror rest along with the support structure is designed in such a way that the mirror centre coincides with the fixed wrist point.

#### 4.2. Control of 3-UPU manipulator

Closed-loop [26, 27] as well as open-loop control strategies [28, 29] have been used for tracking the sun as it moves across the sky. The closed-loop strategies require the use of CCD cameras or other external sensors which can be used for feedback and control. This increases cost and as a result the current industrial norm is open-loop tracking of the sun. The error introduced as a result of open-loop control is reduced by periodic calibration using a target screen situated below the receiver aperture and image processing techniques. For our prototype and proof of concept, we employ open-loop control strategy relying on the predefined apparent motion of the sun from algorithms already developed [30] and feedback from the actuator encoders. The actuators used to actuate the U-joints consist of a DC servo-motor connected to a lead screw. A full rotation of the motor shaft results in 1.5 mm translation, i.e., the pitch of the lead screw

is 1.5 mm. The inertia of the motor, friction and other actuator parameters were not available and hence to obtain a transfer function of the linear actuator and find the actuator parameters, we performed experiments. For the actuator the input was a voltage and the output was the linear distance moved by the actuator. The rotation of the motor was measured from an inbuilt quadrature encoder. The input voltage was provided as a square wave of amplitude 20 V having a period of 10 s and 50 % duty cycle. An H-bridge was used to reverse the motion of the actuator. We have used the system identification tool box in Matlab [31] to estimate the transfer function of the linear actuator. Typically

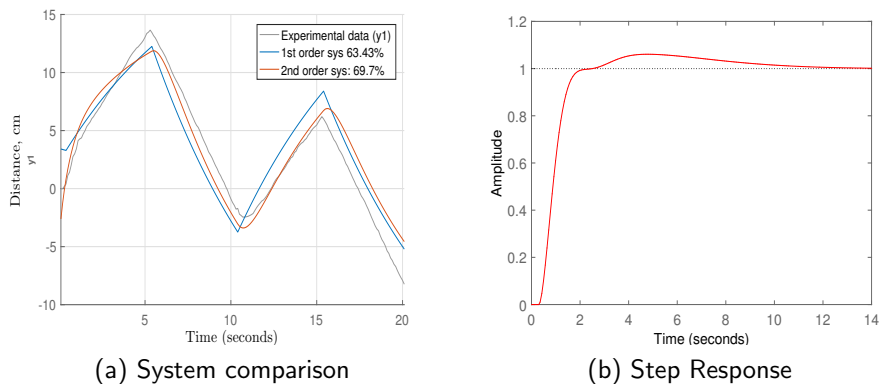


Fig. 11: System identification using Matlab-Simulink

the modeling of a permanent magnet DC motor is done using equations given by

$$L_a \dot{I}_a + R_a I_a = V - K \dot{\theta} \quad (9)$$

$$J \ddot{\theta} + b \dot{\theta} = K I_a \quad (10)$$

where  $L_a$ ,  $R_a$  are the inductance and resistance of the armature,  $K$  is a constant,  $I_a$  is the current flowing through the armature,  $V$  is the voltage applied,  $J$  is the inertial of the rotor,  $b \dot{\theta}$  denotes the dissipation with  $\dot{\theta}$  denoting the angular velocity of the rotor. The transfer function obtained from the above equations, by using the standard Laplace transform technique, would be third-order. If we make the often performed simplifying assumption that the inductance is small, the system becomes a second-order. Fig 11a gives the plot of experimental data (the encoder pulses were converted to linear distance traversed by multiplying with a constant) versus the first-order as well as the second-order system. It can be seen that the second-order system is more in accordance with the experimental data. The transfer function thus obtained using the system identification

toolbox of Matlab [] is given by Eqn. (11) below

$$H(s) = \exp^{-0.3s} \frac{0.2504}{s^2 + 1.759s + 0.2766} \quad (11)$$

260 It may be noted that the system identification results in an exponential term,  $\exp^{-0.3s}$ . This arises due to a delay between the given input and the output.

For this transfer function, a PID controller was developed using Matlab-Simulink [31] with a first-order filter on the derivative term as shown in Eqn. (12) below

$$V(s) = K_p + \frac{K_i}{s} + K_d \frac{s}{1 + sT_f} \quad (12)$$

From the experimental data and the system identification tool box, the value of the constants found out are  $K_p = 6.43$ ,  $K_i = 1.78$ ,  $K_d = 4.34$ ,  $T_f = 0.183$  and the step response plot for the estimated second-order system is shown in Fig 11b.

265 The tracking of the sun and reflecting the incident sun rays to the receiver is carried out in discrete time intervals. In the PID controller, a settling time of 11 s (??? is it 11 s can we write 10 s???) is used since the idle time between any two tracking instants would generally be in minutes. Once the system transfer function is obtained, we performed experiments on a roof top with the fabricated 3-UPU based heliostat. For the actual experiments, the co-ordinates of the centre of the receiver is at  $[0 \ 0 \ 6.72]^T$  m with respect to the global co-ordinate system. The origin of the base co-ordinate system is at  $[-10 \ 3 \ 0]^T$  m. For these chosen parameter values the translation at the P joints (or the translation of the linear actuators) required to track the sun for May 24, 2017 at Bangalore using the Az-El and the T-A methods (see section 2.3) is shown in Fig 12. The values of the leg lengths are the desired commands to an ATmega2560 micro-controller used to control the motion of the three actuators.

270 Fig 13 shows the image formed on the receiver wall for two time instants for both the Az-El and T-A heliostats. As it can be seen from Fig 13, the 3-UPU based heliostat is able to track the sun in the Az-El and T-A mode. It can be seen that the two images on the receiver are separated and the difference in their location is somewhat large although the time interval between them is not very large. We discuss the possible sources of error in the next section.

### 285 4.3. Observations and discussions

One of the main problem with the sun tracking experiments carried out on the roof is that the fixed point on the heliostat is not exactly at 866 mm from the base, i.e., the fabricated 3-UPU is not a perfect wrist. This is the primarily reason that the reflected image on the receiver is not at the aim point which is at the centre of the yellow rectangle (at 6.72 m from the global origin). An ideal 3-UPU wrist has only three rotational degrees of freedom but the misalignment of the fixed point due to manufacturing inaccuracies makes the heliostat move in position as well as orientation and this is more difficult to control with our

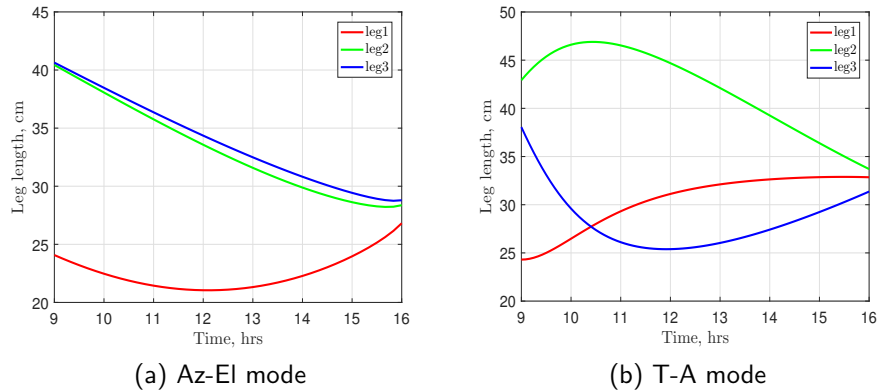


Fig. 12: Leg length required for the 3-UPU wrist to work in Az-El and T-A mode

present controller. A tighter manufacturing tolerance level has to be maintained  
 295 to reduce the errors in pointing.

As mentioned earlier, the sun tracking is done in discrete time intervals. This requires the heliostat to hold on to a particular orientation for a predefined period of time (or the actuators would be idle). During this time, if there are gusts strong enough to cause a change in the orientation of the mirror, the  
 300 control system could not bring it back to its commanded location. This is an additional reason for the somewhat large error in pointing.

In spite of the errors, it can be concluded that the 3-UPU wrist heliostat is able to track the sun in both the Azimuth-Elevation and Target-Aligned mode. It may be mentioned that the switch between the two modes *does not* involve  
 305 any hardware changes and can be simply done in software. In this sense, the 3-UPU based heliostat is reconfigurable and can be used in a mode where the spillage losses and astigmatic aberrations can be minimized.

## 5. Conclusions and future work

The major advantages of using a parallel manipulator as heliostats lie in  
 310 its inherent ability to position the end-effector (mirror) more accurately thus improving the tracking accuracy when compared to serial mechanisms. A parallel manipulator is also known to be more stiffer, allowing it to carry larger mirrors or requiring less structural supporting members to reduce deformation due to wind and self-weight, thereby resulting in cost reduction. Finally, one  
 315 can substitute rotary actuators and expensive speed reducers with simpler and cheaper linear actuators. This work presents the kinematic analysis, control and experimental validation of a novel 3-UPU wrist parallel manipulator as a heliostat in central receiver concentrated solar power systems. The existence of a fixed point for the 3-UPU wrist enables it to be used as a traditional Azimuth-  
 320 Elevation (Az-El) or a Target aligned (T-A) heliostat by changing the control





(a) Az-EL 3:18 p.m.



(b) T-A 3:20 p.m.



(c) Az-EL 3:45 p.m.



(d) T-A 3:48 p.m.

Fig. 13: The image on the receiver at various time instants

strategy alone and with no change in the hardware. The spillage losses can be minimized by switching from the Az-EL to T-A or vice-versa when required. Extensive simulations have been carried out and this fact has been verified. The numerical simulations have been validated using a prototype 3-UPU wrist manipulator based heliostat.

325

The future work includes making a prototype with tighter manufacturing tolerances which will reduce the pointing errors as well as address the requirement of better control. Simulations for other potential locations on the surface of Earth and for various other days need to be carried out. Finally, instead of the two configurations, rotations of the mirror about two arbitrary but independent axis can also be attempted to investigate if there are other better ways to use the available redundant one degree of freedom in the 3-UPU wrist manipulator.

330

## References

- [1] V. Gough, Contribution to discussion of papers on research in automobile stability, control and tyre performance, in: Proc. Auto Div. Inst. Mech. Eng, Vol. 171, 1956, pp. 392–394. 335
- [2] D. Stewart, A platform with six degrees of freedom, Proceedings of the Institution of Mechanical Engineers **180** (1), 1965, pp. 371–386.
- [3] J.-P. Merlet, Parallel robots, Vol. 74, Springer Science & Business Media, 2012. 340
- [4] L. Vant-Hull, Concentrating solar power technology: Principles, developments and applications, Woodhead Publishing, Cambridge, UK, 2012, Ch. 8, pp. 240–283.
- [5] A. Pfahl, J. Coventry, M. Röger, F. Wolfertstetter, J. F. Vásquez-Arango, F. Gross, M. Arjomandi, P. Schwarzbözl, M. Geiger, P. Liedke, Progress in Heliostat Development, Solar Energy (In press, accepted manuscript), 2017. 345
- [6] A. Cammarata, Optimized design of a large-workspace 2-dof parallel robot for solar tracking systems, Mechanism and Machine Theory, **83**, 2015, pp. 175–186. 350
- [7] O. Altuzarra, E. Macho, J. Aginaga, V. Petuya, Design of a solar tracking parallel mechanism with low energy consumption, Proceedings of the Institution of Mechanical Engineers, Part C: Journal of Mechanical Engineering Science, 2014, 0954406214537249.
- [8] Google Inc., Heliostat cable actuation system design, Mountain View, California. 355
- [9] W. Li, J. Sun, J. Zhang, K. He, R. Du, A novel parallel 2-dof spherical mechanism with one-to-one input-output mapping., WSEAS Transactions on Systems, **5** (6), 2006, pp. 1343–1348.
- [10] C. M. Gosselin, F. Caron, Two degree-of-freedom spherical orienting device, US Patent 5,966,991, October 1999. 360
- [11] M. Ruggiu, Kinematic and dynamic analysis of a two-degree-of-freedom spherical wrist, Journal of Mechanisms and Robotics, **2** (3), 2010, pp. 031006.
- [12] M. Carricato, V. Parenti-Castelli, A novel fully decoupled two-degrees-of-freedom parallel wrist, The International Journal of Robotics Research, **23** (6), 2004, pp. 661–667. 365
- [13] B.-H. Lim, K.-K. Chong, C.-S. Lim, A.-C. Lai, Latitude-orientated mode of non-imaging focusing heliostat using spinning-elevation tracking method, Solar Energy, 135, 2016, pp. 253–264. 370

- [14] T. Ashley, E. Carrizosa, E. Fernández-Cara, Optimisation of aiming strategies in solar power tower plants, *Energy* (In press, accepted manuscript), 2017.
- [15] M. J. Lindberg V., Skf dual axis solar tracker-from concept to product, Chalmers University, Sweden, 375
- [16] J. Freeman, B. Shankar, G. Sundaram, Inverse kinematics of a dual linear actuator pitch/roll heliostat, in: *AIP Conference Proceedings*, Vol. 1850, AIP Publishing, 2017, p. 030018.
- [17] M. Balz, V. Göcke, T. Keck, F. von Reeken, G. Weinrebe, M. Wöhrbach, Stello-development, construction and testing of a smart heliostat, in: *AIP Conference Proceedings*, Vol. 1734, AIP Publishing, 2016, p. 020002. 380
- [18] F. Arbes, G. Weinrebe, M. Wöhrbach, Heliostat field cost reduction by slope drive optimization, in: *AIP Conference Proceedings*, Vol. 1734, AIP Publishing, 2016, p. 160002.
- [19] R. A. Shyam, A. Ghosal, Three-degree-of-freedom parallel manipulator to track the sun for concentrated solar power systems, *Chinese Journal of Mechanical Engineering*, **28** (4), 2015, pp. 793–800. 385
- [20] M. Karouia, J. Hervé, A three-dof tripod for generating spherical rotation, in: *Advances in Robot Kinematics*, Springer, 2000, pp. 395–402.
- [21] R. Di Gregorio, Kinematics of the 3-UPU wrist, *Mechanism and Machine Theory*, **38** (3), 2003, pp. 253–263. 390
- [22] Y. Chen, K. Chong, T. Bligh, L. Chen, J. Yunus, K. Kannan, B. Lim, C. Lim, M. Alias, N. Bidin, et al., Non-imaging, focusing heliostat, *Solar Energy*, **71** (3), 2001, pp. 155–164.
- [23] X. Wei, Z. Lu, W. Yu, H. Zhang, Z. Wang, Tracking and ray tracing equations for the target-aligned heliostat for solar tower power plants, *Renewable Energy* **36** (10), 2011, pp. 2687–2693. 395
- [24] M. Guo, Z. Wang, W. Liang, X. Zhang, C. Zang, Z. Lu, X. Wei, Tracking formulas and strategies for a receiver oriented dual-axis tracking toroidal heliostat, *Solar Energy*, **84** (6), 2010, pp. 939–947. 400
- [25] A. Ghosal, *Robotics Fundamental Concepts and Analysis*, Oxford University Press, New Delhi, India, 2006.
- [26] M. Chiesi, E. F. Scarselli and R. Guerrieri, Run-time detection and correction of heliostat tracking errors, *Renewable Energy*, **105**, 2017, pp. 702–711. 405

- [27] F. J. Delgado, J. M. Quero, J. Garcia, C. L. Tarrida, P. R. Ortega, S. Bermejo, Accurate and wide-field-of-view mems-based sun sensor for industrial applications, *IEEE Transactions on Industrial Electronics* **59** (12), 2012, pp. 4871–4880.
- 410 [28] R. Baheti, P. Scott, Design of self-calibrating controllers for heliostats in a solar power plant, *IEEE Transactions on Automatic Control* **25** (6), 1980, pp. 1091–1097.
- [29] S. A. Jones, K. Stone, Analysis of solar two heliostat tracking error sources, Tech. rep., Sandia National Laboratories, Albuquerque, NM, and Livermore, CA, 1999.
- 415 [30] W. B. Stine, M. Geyer, *Power from the Sun*, Power from the sun. net, 2001.
- [31] Matlab R2015a, 64bit version, Mathworks Inc., Natick Massachussets, 2015.